# Self-assembled nanostructured ZnO hollow spheres with UVA luminescence

**H. Arami, M. Mazloumi, R. Khalifehzadeh and S. K. Sadrnezhaad***

Nanostructured ZnO hollow spheres with average crystallite size of ~50 nm, particle size distribution in the range of 600–2000 nm and a typical shell thickness of about 300–700 nm, were successfully fabricated through a facile hydrothermal route, using triethanolamine (TEA, $C_6H_{15}NO_3$) as a morphology control agent and pH as the structural involved parameter. Hollow spheres were formed due to self-assembled aggregation of zinc ion complexes and formation of internal voids with Ostwald ripening mechanism. These internal spaces can be filled and the spheres may enlarge, due to diffusion of the ionic complexes of the solution toward the surface of the initial particles and Kirkendall effect. This phenomenon was supposed to cause the mentioned size distribution in the outer diameters of the hollow spheres and their internal voids. The fabricated nanostructured spheres showed an ultraviolet A (UVA) luminescence and an intense yellow emission in the visible band which can be attributed to the low density of oxygen defects on the surface of the synthesised particles.

**Keywords:** Nanostructures, Oxide, Chemical synthesis, Defects, Luminescence

## Introduction

Zinc oxide (ZnO) is a versatile semiconducting material with a wide and direct band gap (3·37 eV) and large exciton binding energy (60 meV),[1] which results in efficient excitonic emission at room temperature and unique optical, acoustic, electronic,[2] catalytic and photocatalytic properties,[3] which make it a relevant choice for optoelectric devices,[4] solar cells,[5] sensors,[6] varistors and electroluminescent devices.[1] Various morphologies with different properties were reported previously for ZnO nanostructures, such as nanotubes,[7] nanowires,[8] nanorods[9] and flowerlike nanoarchitectures.[10]

The ability of nanoparticles to self-assemble into well defined configurations in space is becoming increasingly important due to their novel applications in nanoscience and nanotechnology.[11,12] Self-organising synthesis refers to an assembly of single molecules, biomolecules or complex molecular clusters in a predesigned pattern with control over molecular spacing, orientation and interaction. In self-assembly, the components explore the space of possible molecular orientations and if some particular arrangement is more stable, it will be preferred and adapted.[13] Such assembly relies on weak non-covalent bonds, such as ionic bonds, hydrogen bonds, hydrophobic and van der Waals interactions.[14] Shape complementarity, which can be determined by positioning and size of functional groups, plays a dominant role in the final shape and stoichiometry of the assembled architectures.[15] Such autonomous arrangements can be applied to fabricate hierarchically structures through mechanisms such as cooperative,[16] kinetic[17] or biomimetic[18] self-assembly and methods such as electrosprays or electrohydrodynamic jet[19,20] assembly, to build increasingly complex micro- and nanostructures, such as hollow nanostructures,[17,21] micelles, films, membranes, tubes, rods, mesophases and nanoparticles.[22,23] In addition, a concept of 'molecular Lego' based on a different set of structural elements, was proposed and developed by Stoddard *et al.*,[24,25] which belongs to the wider category of 'modular chemistry' in which a small number of mid sized rigid molecular structural components are combined into complex structures.

Hollow nanomaterials can be produced via two main strategies: template assisted synthesis via utilisation of removable or sacrificial templates[26–28] and template free synthesis through various physicochemical processes such as Kirkendall effect,[29] Ostwald ripening[30] and hydrophobic interactions.[31] Some efforts have recently been made to synthesise hollow ZnO structures with outstanding potential applications in electronics, optoelectronics, complex hierarchical assemblies[32] and drug delivery[33] for their low densities, high surface areas, biocompatibility[34] and unique optical, electrical and surface properties.[35]

In this paper, the authors introduce a facile hydrothermal route for self-assembly fabrication of nanostructured ZnO hollow spheres with the help of triethanolamine (TEA) and pH effect. Previously, Pal and Santiago[36] have shown that ZnO morphologies were strongly dependent on the initial and final pH of the solution during low temperature hydrothermal synthesis of ZnO nanostructures.

Materials and Energy Research Center, PO Box 14155-4777, Tehran, Iran

*Corresponding author, email sadrnezh@sharif.edu


Published by Maney on behalf of the Institute
Received 26 November 2006; accepted 1 February 2007
DOI 10.1179/174367607X202609

It is reported that physical, electronic, optical and chemical properties of semiconducting nanomaterials can be improved remarkably by engineering the band gap[5] and preparation conditions.[2,35] The photoluminescence (PL) technique has been extensively used to investigate the surface characteristics and structure of metal oxides.[3] In this investigation, the authors have also utilised room temperature photoluminescence (RT-PL) spectroscopy to characterise the optical and structural properties of nanostructured ZnO hollow spheres.

## Experimental

The details of materials together with their sources are given in Table 1. All the materials were used as received without further purification. In a typical synthesis method, a mixture of 80 cc water and 10 vol.-%TEA ($C_6H_{15}NO_3$) was poured into a double neck 100 cc round bottom flux. TEA was used as a pH adjuster and emulsifying surfactant. The pH of the water and TEA mixture was ~10·5. Zinc acetate dehydrate [$(CH_3COO)_2Zn.2H_2O$] crystals were added to the solvent under vigorous agitation until the desired $pH_i$=9 was reached. After the zinc acetate was dissolved completely, potassium hydroxide (KOH) pellets were added to the mixture to increase the pH of the mixture to 10. The resulting solutions were then transferred into Teflon lined stainless steel autoclaves. The autoclaves were sealed and maintained at 100°C for 2 h. After the reaction was completed, the autoclave was allowed to cool to room temperature naturally. The solid white precipitates were filtered, washed several times with deionised water to remove impurities and then dried at 55°C in air. The obtained white powders were characterised with scanning electron microscopy (SEM, Philips XL30, Eindhoven, The Netherlands), transmission electron microscopy (TEM, Philips CM200, Eindhoven, The Netherlands), X-ray diffraction analysis (XRD, Philips X'Pert diffractometer, Eindhoven, The Netherlands) and RT-PL (Perkin-Elmer, LS-5 spectrofluorimeter, Norwalk, CT, USA) equipped with a xenon discharge lamp.

## Results and discussion

ZnO (wurtzite) belongs to the space group of $P6_3mc$ (no. 186), with cell constants $a$=3·24 Å, $c$=5·20 Å and the hexagonal symmetry. The major axis is symmetrically polar and results in a hemimorphic crystal structure. As shown in Fig. 1, the obtained powder was composed of ZnO particles with high crystallinity and wurtzite crystal structure. All the XRD peaks (Fig. 1) were indexed and they agreed with the standard ZnO of hexagonal structure (JCPDS Card no. 36-1451). No characteristic peaks were observed for the other phases and impurities. The average crystallite size of the particles was determined to be ~50 nm, using Scherrer formula

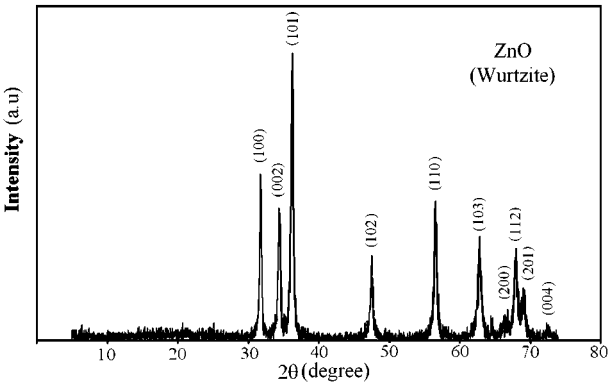


**1 X-ray diffraction pattern of obtained powder: all peaks were indexed according to JCPDS Card no. 36-1451**

$$d = \frac{K\lambda}{B\cos\theta}$$

where $d$ is the crystallite size of the powder, $\lambda$ is the wavelength of Cu $K_\alpha$ (1·54056 Å), $B$ is the full width at half maximum intensity of the peak in radian, $\theta$ is Bragg's diffraction angle and $K$ is a constant usually equal to ~0·9.[37]

Scanning electron images (Fig. 2) reveal nanostructured ZnO spheres in the size range of 600–2000 nm. It can be clearly seen that there is a size distribution among the obtained spheres. The porosities on the surface of the spheres (Fig. 2*b*) can be the gateway for material transportation, i.e. drug delivery[38] or gene delivery systems,[39] as the materials could penetrate inside these spheres and then diffuse out into the desired location. Although most of the spheres were observed to have a closed shell, a typical image of an open single hollow sphere with average diameter of 1·12 μm and shell thickness of ~300 nm is provided to confirm the hollow structure of the spheres (Fig. 2*c*) with a uniform shell thickness. Even though, wurtzite (ZnO) crystal structure is polar with different growth rates of the crystal planes, i.e. $(0001)>(10\bar{1}\bar{1})>(\bar{1}010)>(\bar{1}011)>(000\bar{1})$, which determine the crystal morphology;[40] the spherical ZnO particles will easily grow due to the Ostwald ripening process[10,41] and the utilised solvent,[40] in order to decrease their interfacial free energy.

As self-assembly has been introduced as a collection and aggregation of molecular components into a confined entity by pioneers like Lehn,[42] the possible mechanism for the fabrication of ZnO hollow spheres in this investigation is based on self-assembled aggregation of $Zn^+$ ion complexes due to ionic bonding between amine groups of TEA and the negatively charged acetate ions ($CH_3COO^-$)[43] and subsequent evacuation through Ostwald ripening to produce a void[21] (Fig. 3). Beside Ostwald ripening process, chemical conditions affect the growth of the ZnO particles. Previous research revealed that morphologies, such as hollow spheres, could be

**Table 1 Details and sources of materials**

| Material | Supplier | Molar weight, g mol$^{-1}$ |
|---|---|---|
| Triethanolamine (TEA, $C_6H_{15}NO_3$) | Merck KgaA, Darmstadt, Germany | 149·19 |
| Zinc acetate dehydrate [$(CH_3COO)_2Zn.2H_2O$] | Merck KgaA, Darmstadt, Germany | 219·49 |
| Potassium hydroxide (KOH) | BDH Laboratory Supplies, Poole, UK | 56·11 |

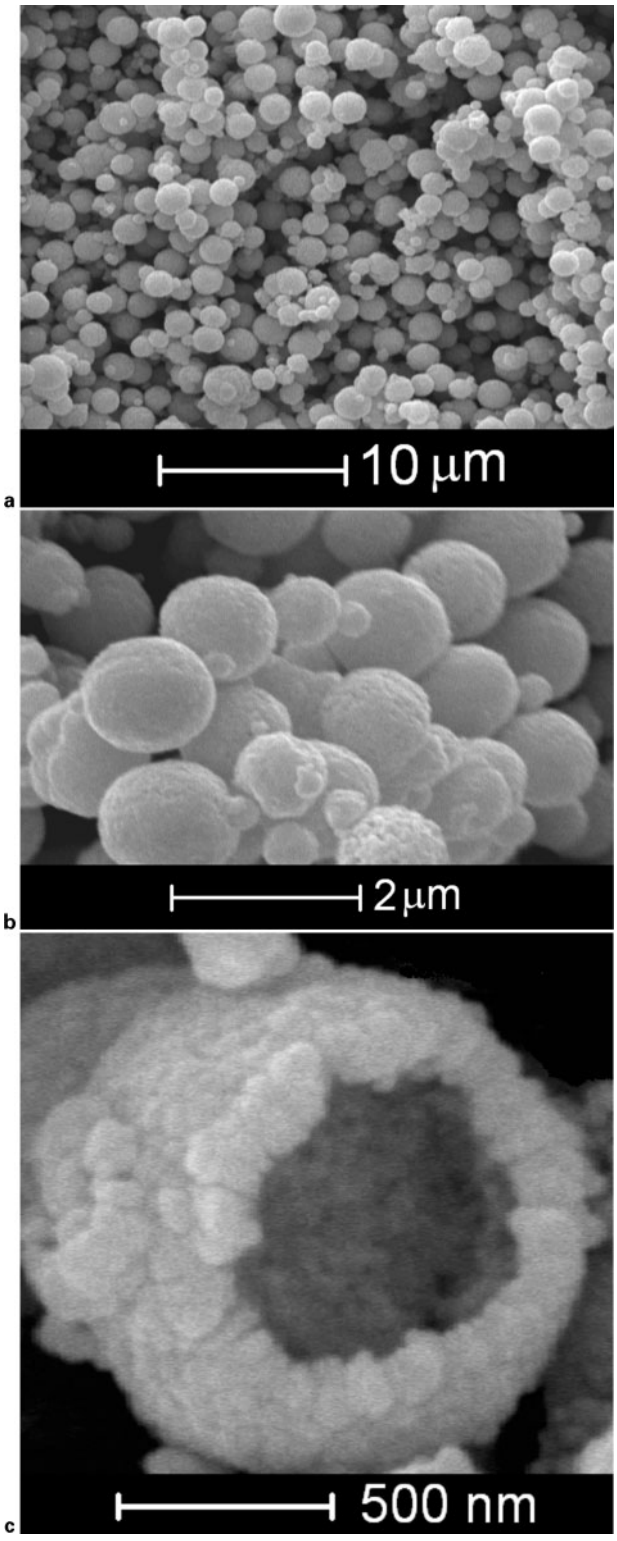


**2 Images (SEM) of nanostructured hollow submicron and microspheres with *a* low and *b* high magnification, and *c* typical nanostructured hollow sphere**

formed by changing the pH of the solution during the formation and decomposition of zinc complexes in the presence of TEA.[44] It was also shown that the shape of the nanostructure was independent of the decomposition pH which affected the formation rate and size of the ZnO particles. In addition, initial pH affected the nature of the zinc complex generated during the process.[44]

Subsequent self-aggregation of zinc ion complexes onto the sphere surface caused to randomly thicken the

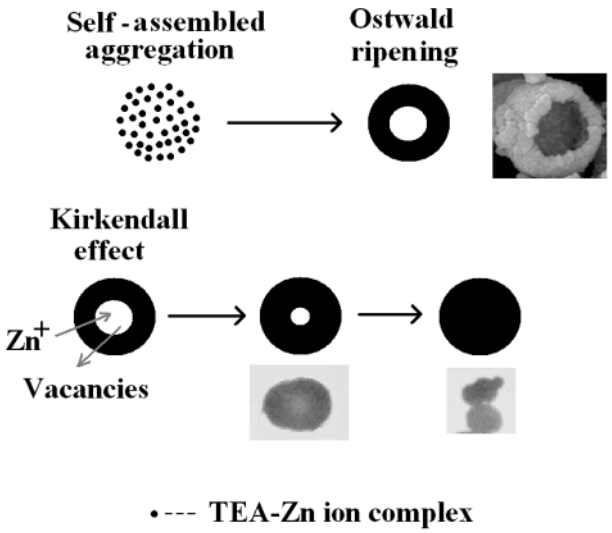


**3 Schematic of possible self-assembly mechanism for formation of ZnO hollow spheres and subsequent filling process**

shell exteriorly and resulted in a size distribution (Fig. 2*a*). Simultaneously, the mutual diffusion of internal vacancies outward and the fast moving zinc ions in the vicinity of the sphere interface inward via Kirkendall effect,[29] culminated in filling the internal spaces in some spheres (Fig. 3). The presence of filled (A) and hollow (B) particles can be observed in the TEM image (Fig. 4). As shown, there are some typical filled spheres together with hollow ones in the image. The observed contrast between the pale centre and the dark edge of the spheres is evidence of this hollow nature. The microspheres did not agglomerate to form multivoids.

The selected area electron diffraction (SAED) of a region in the vicinity of the external edge of an individual sphere is shown in the inset of Fig. 4. The pattern indicates that the direction of the electron beam was along the [0001] zone axis of the selected ZnO nanostructure and the crystal structure of the synthesised material is similar to the wurtzite ZnO hexagonal lattice in accordance with the XRD results (Fig. 1).

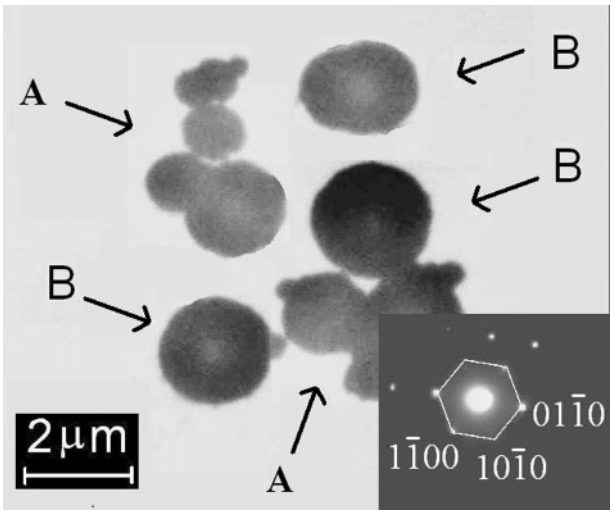


**4 TEM image of nanostructured filled (A) and hollow spheres (B) (μm): inset is selected area electron diffraction (SAED) pattern of region in vicinity of external edge of individual sphere**

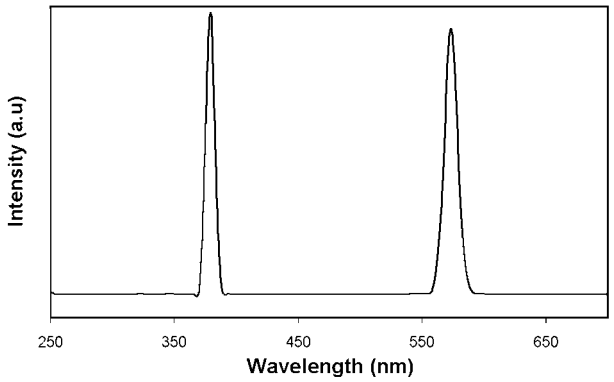


**5 Room temperature photoluminescence (RT-PL) emission spectrum of nanostructured hollow spheres with excitation wavelength of 325 nm**

Important information such as surface defects, oxygen vacancies, surface states, photo induced charge carrier separation and recombination processes in nanosized semiconductor materials can be obtained from a PL spectra.[3] Obtaining PL spectrum is, therefore, an effective way to investigate the electronic structure and optical and photochemical properties of semiconductor materials. Results can lead to crucial information about surface oxygen vacancy, defects and charge efficiency, and immigration and transfer of the trapping carriers.[3]

The RT-PL emission spectrum of the synthesised ZnO spheres determined with an excitation wavelength of 325 nm, is shown in Fig. 5. The intense peak observed at $\sim$370 nm, i.e. the ultraviolet A (UVA) region, can be attributed to the band edge emission[3] by simultaneously releasing the energy as UVA radiation. This is an interesting result, which confirms low density of defects in nanostructured ZnO hollow spheres.[5] A sharp emission was observed $\sim$575 nm in the yellow part of the visible spectrum. The yellow emission has previously been reported to be related to the interstitial negatively charged single oxygen ions ($O_i^-$) in the ZnO crystal structure.[4,36] Visible emission which is generally green is considered to be due to non-stoichiometric composition. Oxygen vacancies ($V_O$), oxygen interstitials ($O_i$) and ionic dopants result in yellow and orange emissions creating different peaks.[1] According to Chen *et al.*,[45] the position of the emission band in the visible region shifts from green to yellow as the density of the oxygen related defects decreases. Hence, as there is just a yellow emission in the visible band, the authors can conclude that these ZnO hollow spheres are highly crystallised, and have outstanding optical quality[41] and a reduced density of oxygen defects. Such reduction in density of defects can be attributed to using a single source precursor [i.e. $(CH_3COO)_2Zn.2H_2O$] that contains preformed Zn–O bonds and could yield ZnO nanocrystals with low defect densities.[5] This phenomenon is of great practical significance, because the oxygen vacancies can enhance the adsorption of $O_2$ and produce active $\bullet O_2$ radical groups to oxidise the organic materials.[3] Therefore, it can be suggested that these low defect density ZnO hollow spheres can be utilised in the delivery of organic substances, such as drugs or other biological molecules, without having them degraded.

## Conclusions

ZnO nanocrystalline hollow spheres with an average crystallite size of $\sim$50 nm, determined by Scherrer formula, particle size distribution in the range of 600–2000 nm and a typical shell thickness of about 300–700 nm, were synthesised using a hydrothermal approach. Self-assembly of zinc ion complexes and amine functional groups of TEA resulted in aggregation of the components to form hollow spheres through Ostwald ripening process. Kirkendall effect culminated in filling of some spheres due to mutual diffusion of zinc ions and vacancies, inward and outward, respectively. Photoluminescence characterisation showed a UVA irradiation at $\sim$370 nm and an intense yellow peak in the visible band. These luminescence peaks revealed the low content of oxygen surface defects in the synthesised material.

## Acknowledgement

The authors sincerely appreciate the reviewer(s) of the manuscript, whose kind and thorough reviews improved the content of this work.

## References

1. H. M. Cheng, K. F. Lin, H. C. Hsu, C. J. Lin, L. J. Lin and W. F. Hsieh: *J. Phys. Chem. B*, 2005, **109B**, 18385–18390.
2. H. S. Qian, S. H. Yu, J. Y. Gong, L. B. Luo and L. L. Wen: *Cryst. Growth Des.*, 2005, **5**, 935–939.
3. L. Q. Jing, Y. C. Qu, B. Q. Wang, S. D. Li, B. J. Jiang, L. B. Yang, W. Fu, H. G. Fu and J. Z. Sun: *Sol. Energy Mater. Sol. Cells*, 2006, **90**, 1773–1787.
4. G. Shen, Y. Bando and C. J. Lee: *J. Phys. Chem. B*, 2005, **109B**, 10779–10785.
5. Y. S. Wang, P. J. Thomas and P. O'Brien: *J. Phys. Chem. B*, 2006, **110B**, 4099–4104.
6. J. Németh, G. R. Gattorno, D. Díaz, A. R. V. Olmos and I. Dékány: *Langmuir*, 2004, **20**, 2855–2860.
7. Q. Li, V. Kumar, Y. Li, H. Zhang, T. J. Marks and R. P. H. Chang: *Chem. Mater.*, 2005, **17**, 1001–1006.
8. G. S. Wu, T. Xie, X. Y. Yuan, Y. Li, L. Yang, Y. H. Xiao and L. D. Zhang: *Solid State Commun.*, 2005, **134**, 485–489.
9. B. Liu and H. C. Zeng: *Langmuir*, 2004, **20**, 4196–4204.
10. X. Gao, X. Li and W. Yu: *J. Phys. Chem. B*, 2005, **109B**, 1155–1161.
11. G. M. Whitesides and B. Grzybowski: *Science*, 2002, **295**, 2418–2421.
12. J.-M. Lehn: *Angew. Chem. Int. Ed. Engl.*, 1988, **27**, 89–112.
13. R. C. Merkle: *Trends Biotechnol.*, 1999, **17**, 271–274.
14. G. M. Whitesides, J. P. Mathias and C. T. Seto: *Science*, 1991, **254**, 1312–1319.
15. K. P. McGrath and M. M. Butler: in 'Protein-based materials', (ed. K. McGrath and D. Kaplan), 251– 279; 1997, Boston, MA, Birkhauser.
16. P. Yang, T. Deng, D. Zhao, P. Feng, D. Pine, B. F. Chmelka, G. M. Whitesides and G. D. Stucky: *Science*, 1998, **282**, 2244–2246.
17. J. Wang, Q. Xiao, H. Zhou, P. Sun, Z. Yuan and B. Li: *Adv. Mater.*, 2006, **18**, 3284–3288.
18. A. Firouzi, D. Kumar, L. M. Bull, T. Besier, P. Sieger, Q. Huo, S. A. Walker, J. A. Zasadzinski, C. Glinka, J. Nicol, D. I. Margolese, G. D. Stucky and B. F. Chmelka: *Science*, 1995, **267**, 1138–1143.
19. S. N. Jayasinghe: *Physica E*, 2006, **31E**, 17–26.
20. S. N. Jayasinghe and A. C. Sullivan: *J. Phys. Chem. B*, 2006, **110B**, 2522–2528.
21. J. J. Teo, Y. Chang and H. C. Zeng: *Langmuir*, 2006, **22**, 7369–7377.
22. S. I. Stupp, V. LeBonheur, K. Walker, L. S. Li, K. E. Huggins, M. Keser and A. Amstutz: *Science*, 1997, **276**, 384–389.
23. G. Decher: *Science*, 1997, **277**, 1232–1237.
24. F. Stoddard: *Chem. Brit.*, 1988, **24**, 1203–1208.
25. F. M. Raymo and J. F. Stoddart: *Chem. Rev.*, 1999, **99**, 1643–1664.

26. S. Gao, H. Zhang, X. Wang, R. Deng, D. Sun and G. Zheng: *J. Phys. Chem. B*, 2006, **110B**, 15847–15852.
27. C. Yan and D. Xue: *J. Phys. Chem. B*, 2006, **110B**, 7102–7106.
28. H. Kou, J. Wang, Y. Pan and J. Guo: *Mater. Chem. Phys.*, 2006, **99**, 325–328.
29. Y. Yin, R. M. Rioux, C. K. Erdonmez, S. Hughes, G. A. Somorjai and A. P. Alivisatos: *Science*, 2004, **304**, 711–714.
30. Y. Zheng, Y. Cheng, Y. Wang, L. Zhou, F. Bao and C. Jia: *J. Phys. Chem. B*, 2006, **110B**, 8284–8288.
31. S. Park, J.-H. Lim, S.-W. Chung and C. A. Mirkin: *Science*, 2004, **303**, 348–351.
32. S. Ravindran, G. T. S. Andavan and C. Ozkan: *Nanotechnology*, 2006, **17**, 723–727.
33. J. Duan, X. Huang, E. Wang and H. Ai: *Nanotechnology*, 2006, **17**, 1786–1790.
34. J. Zhou, N. Xu and Z. L. Wang: *Adv. Mater.*, 2006, **18**, 2432–2435.
35. H. M. Cheng, H. C. Hsu, S. L. Chen, W. T. Wu, C. C. Kao, L. J. Lin and W. F. Hsieh: *J. Cryst. Growth*, 2005, **277**, 192–199.
36. U. Pal and P. Santiago: *J. Phys. Chem. B*, 2005, **109B**, 15317–15321.
37. B. D. Cullity: 'Elements of X-ray diffraction', 2nd edn; 1978, London, Addison-Wesley.
38. Q. Liu, H. Liu, M. Han, J. Zhu, Y. Liang, Z. Xu and Y. Song: *Adv. Mater.*, 2005, **17**, 1995–1999.
39. Z. L. Wang: *Mater. Today*, 2004, **7**, 26–33.
40. T. Andelman, Y. Gong, M. Polking, M. Yin, I. Kushovsky, G. Neumark and S. O'Brien: *J. Phys. Chem. B*, 2005, **109B**, 14314–14318.
41. L. Xu, Y. Guo, Q. Liao, J. Zhang and D. Xu: *J. Phys. Chem. B*, 2005, **109B**, 13519–13522.
42. J.-M. Lehn: *Proc. Natl Acad. Sci. USA*, 2002, **99**, 4763–4768.
43. Y. Hu, X. Jiang, Y. Ding, Q. Chen and C. Yang: *Adv. Mater.*, 2004, **16**, 933–937.
44. A. Eftekhari, F. Molaei and H. Arami: *Mater. Sci. Eng. A*, 2006, **A437**, 446–450.
45. J. Chen, Z. Feng, P. Ying, M. Li, B. Han and C. Li: *Phys. Chem. Chem. Phys.*, 2004, **6**, 4473–4479.